applied sciences

MDPI

Article

Optimizing Energy Efficiency and Sustainability in Winter Climate Control: Innovative Use of Variable Refrigerant Flow (VRF) Systems in University Buildings

Yolanda Arroyo Gómez [1,2,3,*], Julio F. San José-Alonso [1,3,4], Luis J. San José-Gallego [5], Javier M. Rey-Hernández [1,6], Ascensión Sanz-Tejedor [1,2,3] and Francisco J. Rey-Martínez [1,3,4]

1 GIRTER Research Group, Consolidated Research Unit (UIC053) of Castile and Leon, 47011 Valladolid, Spain; julio.sanjose.alonso@uva.es (J.F.S.J.-A.); jrey@uma.es (J.M.R.-H.); atejedor@uva.es (A.S.-T.); rey@uva.es (F.J.R.-M.)
2 Department of Organic Chemistry, ITAP, School of Industrial Engineering, University of Valladolid, Street Doctor Mergelina, s/n, 47011 Valladolid, Spain
3 ITAP Research Institute, University of Valladolid, 47011 Valladolid, Spain
4 Department of Energy and Fluid Mechanics, Engineering School (EII), University of Valladolid, Paseo del Cauce 59, 47011 Valladolid, Spain
5 Solar Energy Institute, Polytechnic University of Madrid, Street Nikola Tesla, 28031 Madrid, Spain; luisjavier.sanjose@upm.es
6 Department of Mechanical Engineering, Fluid Mechanics and Thermal Engines, Engineering School, University of Malaga (UMa), 29016 Málaga, Spain
* Correspondence: yolanda.arroyo@uva.es

Abstract: This study presents a comprehensive analysis of the energy efficiency and sustainability of Variable Refrigerant Flow (VRF) systems in university buildings during the winter season, offering significant contributions to the field. A novel methodology is introduced to accurately assess the real Seasonal Coefficient of Performance (SCOP) of VRF systems, benchmarked against conventional Heating, Ventilation, and Air Conditioning (HVAC) technologies, such as natural gas-fueled boiler systems. The findings demonstrate outstanding seasonal energy performance, with the VRF system achieving a SCOP of 5.349, resulting in substantial energy savings and enhanced sustainability. Key outcomes include a 67% reduction in primary energy consumption and a 79% decrease in greenhouse gas emissions per square meter when compared to traditional boiler systems. Furthermore, VRF systems meet 83% of the building's energy demand through renewable energy sources, exceeding the regulatory SCOP threshold of 2.5. These results underscore the transformative potential of VRF systems in achieving nearly Zero-Energy Building (nZEB) objectives, illustrating their ability to exceed stringent sustainability standards. The research emphasizes the strategic importance of adopting advanced HVAC solutions, particularly in regions with high heating demands, such as those characterized by continental climates. VRF systems emerge as a superior alternative, optimizing energy consumption while significantly reducing the environmental footprint of buildings. By contributing to global sustainable development and climate change mitigation efforts, this study advocates for the widespread adoption of VRF systems, positioning them as a critical component in the transition toward a sustainable, zero-energy building future.

Keywords: seasonal energy efficiency; Variable Refrigerant Flow (VRF); sustainable HVAC; nearly Zero-Energy Building (nZEB); renewable energy integration; climate change mitigation; greenhouse gas (GHG) emissions

Academic Editor: Maria Vicidomini

Received: 20 January 2025
Revised: 18 February 2025
Accepted: 21 February 2025
Published: 23 February 2025

Citation: Arroyo Gómez, Y.; San José-Alonso, J.F.; San José-Gallego, L.J.; Rey-Hernández, J.M.; Sanz-Tejedor, A.; Rey-Martínez, F.J. Optimizing Energy Efficiency and Sustainability in Winter Climate Control: Innovative Use of Variable Refrigerant Flow (VRF) Systems in University Buildings. *Appl. Sci.* **2025**, *15*, 2374. https://doi.org/10.3390/app15052374

1. Introduction

The transition to zero-emission buildings is a critical objective for the European Union (EU), with the target year set for 2050 to eliminate reliance on fossil fuels [1]. Currently, buildings in Europe account for approximately one-third of greenhouse gas emissions and consume 42% of power consumption [2]. To address the challenges associated with energy efficiency and sustainability in the built environment, the European Union has introduced a series of legislative measures; notably, Directive (EU) 2018/844 and, more recently, the 2024 European Parliament legislative resolution on the energy performance of buildings. These directives aim to establish a comprehensive regulatory framework to enhance energy efficiency, reduce carbon emissions, and support the transition towards a more sustainable and resilient built environment across EU member states. By implementing these measures, the EU seeks to ensure the alignment of energy performance standards with the broader objectives of decarbonization and climate change mitigation [3–5].

To achieve these targets, EU policies mandate member states to adopt mechanisms such as Energy Performance Certificates (EPCs), minimum efficiency standards for Heating, Ventilation, and Air Conditioning (HVAC) systems, and financial incentives for renewable energy integration, insulation upgrades, and modernization of outdated equipment [3].

Concurrently, national strategies have increasingly integrated Urban Building Energy Models (UBEMs) and Building Information Modeling (BIM) to create comprehensive databases, such as Spain's HULC 2.0.2496.1177 Software [6], which catalogs energy data for over 1.2 million buildings [7].

Literature Review

The optimization of energy efficiency and sustainability in building operations has been extensively studied through established frameworks, such as the Building Research Establishment Environmental Assessment Methodology (BREEAM) [8]) and Leadership in Energy and Environmental Design (LEED) [9]. Comparative analyses of these methodologies have identified their respective strengths and limitations, particularly in terms of regional adaptability and cost effectiveness [10–12]. Gurgun et al. examined strategies for achieving LEED certification across 1500 buildings in the United States, providing insights into optimizing certification processes to align with project owner expectations [13]. Recent advancements have introduced BIM tools designed to evaluate LEED credits for diverse construction alternatives, enhancing the accuracy of sustainability assessments [14,15].

HVAC technologies, particularly heat pumps (HPs) and Variable Refrigerant Flow (VRF) systems, have emerged as key solutions for minimizing energy consumption and enhancing sustainability in buildings [16]. VRF systems, known for their adaptability and efficiency under varying load conditions, have been extensively analyzed through energy modeling, performance optimization, and predictive analytics. Zhao et al. employed Artificial Neural Networks (ANNs), Support Vector Machines (SVMs), and Auto-Regressive Integrated Moving Average (ARIMA) models to predict VRF system energy consumption in office buildings, determining that ANN-based models exhibited the highest predictive accuracy [17].

Economic feasibility studies by Pallis et al. emphasize the cost effectiveness of VRF/heat pump solutions in five-story office buildings in Greece, showcasing their role in achieving cost optimality and nearly Zero-Energy Building (nZEB) status. The integration of Photovoltaics (PVs) was found to be crucial for reaching nZEB thresholds, with VRF systems playing a pivotal role in achieving sustainability goals [18].

Further experimental and simulation-based research by Wang et al. on Variable Water Volume (VWV) and Air Source Heat Pump (ASHP) systems demonstrated high seasonal energy efficiency, with Seasonal Performance Factors (SPFs) surpassing 3.0. Their findings

propose system enhancements based on real-time operational data, ensuring optimal HVAC performance [19].

The role of occupancy monitoring in energy optimization has gained increasing attention. Gupta et al. analyzed 2700 residential units in Jaipur (India) to identify determinants influencing EPC ratings [20]. Additional studies have examined discrepancies between BIM-modeled and actual energy consumption data in high-performance buildings [21–23]. Wang et al. provided empirical evidence comparing real versus BIM-predicted energy consumption in a nearly zero-energy office building [24].

Occupancy-driven energy management has been explored by Reveshti et al., who applied artificial neural networks to monitor occupancy rates in an office building in Tehran, Iran, revealing a strong correlation between occupancy levels and energy consumption [25]. Similarly, multi-sensor fusion techniques have achieved a 23.5% reduction in energy usage in an academic office building in Wuhan, China, demonstrating the potential of real-time optimization strategies [26]. Recent simulations by Mashuk et al. incorporating detailed agent movement trajectories into electricity consumption models yielded predictions 19% closer to real-world energy use, highlighting the necessity of high-fidelity occupancy tracking for accurate forecasting [27].

The future of HVAC technology is increasingly centered on HP and VRF systems, with research consistently showcasing their superior energy efficiency and environmental benefits [28–31]. Zhao et al. advanced predictive modeling for VRF energy consumption in office environments [17], while Zhou et al. conducted a comparative analysis between EnergyPlus simulations and empirical consumption data in ongoing research into Seasonal Coefficient of Performance (SCOP) optimization, which has led to the development of dynamic evaporator temperature control mechanisms [32].

Liu et al. investigated the performance of a novel heat recovery VRF system designed to optimize energy conservation while ensuring precise indoor temperature and humidity control [33]. Wang et al. conducted a comprehensive review addressing the inherent modeling challenges of VRF systems, considering dynamic load variations and transient operating conditions [34]. Complementary research by Cao et al. introduced a variable evaporating temperature control strategy to enhance VRF efficiency [35]. Additionally, Oh et al. proposed a machine-learning-driven, catalog-based performance estimation model to improve the predictive accuracy of VRF system operations [36].

Furthermore, research has explored the application of heat pumps (HPs) for energy recovery in ventilation systems, including an examination of how calibrating Variable Refrigerant Flow (VRF) systems can significantly enhance energy efficiency in several climates and highlighting various HP technologies and their integration into building ventilation systems [29,37,38]. They underscore their crucial role in reducing energy consumption and promoting sustainability.

This study builds on these advancements by evaluating the real-world SCOP of VRF systems in university buildings during the winter season, benchmarking their performance against conventional natural gas-fueled boiler systems. The findings underscore the transformative potential of VRF systems in meeting sustainability targets, achieving significant energy savings, and advancing nearly Zero-Energy Building (nZEB) objectives. The insights presented here contribute to support optimizing HVAC strategies for high-performance, energy-efficient buildings, reinforcing the critical role of VRF technology in global climate change mitigation efforts.

2. Methodology

In recent years, energy efficiency in buildings has become an increasingly critical aspect of both environmental and economic sustainability. One of the key performance

indicators for evaluating the efficiency of heating systems is the Seasonal Coefficient of Performance (SCOP), which helps determine the energy efficiency of heating systems throughout a given period. This case study focuses on the analysis of the SCOP for the winter period at a building conditioned by a Variable Refrigerant Flow (VRF) system. By evaluating the heating demand and electricity consumption of the system, this study aims to assess the overall performance of the VRF system in real-world conditions.

2.1. Case Study

B1 and B2 are buildings within the María Zambrano University Campus situated in Segovia, a city in northern Spain, positioned approximately 1000 m above sea level. Segovia is characterized by a continental climate. Both buildings hold an EPC rating of Spanish "A" [3] and operate under the same schedule and activity pattern being universities. The base electricity consumption, attributable to equipment, ventilation, and lighting, is considered independent of climatic conditions and remains constant throughout the study period.

The schedule and occupancy of the campus buildings are as follows.

The opening hours of both buildings are as follows. Winter hours are from 8 a.m. to 10 p.m. (a) During the lecture period, the heating systems are turned on from 6 a.m. to 12 and from 3 p.m. to 6 p.m. (luisjavier.sanjose@upm.esb). During non-lecture periods, the heating systems are turned on from 6 a.m. to 10 a.m.

These university buildings under study were constructed in two phases. Building 1 (B1) was built and commenced operations in 2012, utilizing a Low-Temperature Condensing Boiler (LTCB) for winter climate control and a VRF air conditioning system in a small administrative area of the building. Building 2 (B2) was constructed in a subsequent phase and began operations in 2021, employing VRF for winter climate control. Figures 1 and 2 show some of the energy systems of the buildings under study.

(**a**) (**b**)

Figure 1. Energy systems in B1: (**a**) Low-Temperature Condensing Boiler (LTBC), (**b**) VRF.

(**a**) (**b**) (**c**)

Figure 2. Energy systems in B2: (**a**) VRV, (**b**) VRV central, (**c**) and an Air Handling Unit with a heat exchanger.

B1 has a total built-up area of 11,154 m^2, which is distributed as follows: (i) areas without conditioning, 4118 m^2, (ii) areas conditioned by an HP, 1460 m^2, and (iii) the rest of the building conditioned by an LTCB, 5575 m^2.

Table 1 provides an overview of the main energy-consuming equipment and installations in B1 under study.

Table 1. Main energy-consuming installations in B1.

Installations	Equipment Description
Heat generators	• Two Viessmann Low-Temperature Condensing Boilers, model Vitorond 200, with a power of 630 kW. • VRF: Mitsubishi equipment, model PURY 400, with a cooling capacity of up to 90 kW and a heating capacity of up to 100 kW (EER/COP of 3.55/3.76) and up to 100 kW (EER/COP of 3.55/3.76). • Three MITSUBISHI ELECTRIC model PKZ-50VHAL HPs with a cooling capacity of 4.6 kW and a heating capacity of 5.0 kW (EER/COP of 3.55/3.76). A heating capacity of 5.0 kW (EER/COP of 3.22/3.62).
Distribution networks	• Two pipe hot water networks for radiators and air conditioners consisting of a black steel pipe welded DIN-2440 type and insulated with aluminum-finished glass wool insulation. • Nine GRUNDFOS pumps, models UPSD 65-60/4 F, MAGNA D 40-120 F, TPED 230/4-5, MAGNA-D 50-120F, MAGNA-D 32-120F, MAGNA-D 40-120F, MAGNA-D 50-120F, UPSD 32-100 F220, and CH 2-60. • Supply and extract ductwork with supply grilles of 800 × 300 mm and 600 × 300 mm and extract grilles of 800 × 300 mm and φ 100, 150, and 200 mm. • Ductwork consists of CLIMAVER PLUS R ducts. • A refrigerant network made of copper and insulated with a 36 mm thick elastomeric rubber shell.
Heat delivery equipment	• Roca brand aluminum radiators, model Dubal 450 and 800 mm. • A 25 kW compact unit heater. • Eight outdoor air conditioners with S&P plate heat recovery units, model CADT-DC 45 AH DP horizontal, with a heat battery of 30 kW capable of moving 3880 kW. A heat battery of 30 kW capable of moving 3814 m^3/h with an available pressure of 210 Pa. • Underfloor heating with WIRSBO brand cross-linked polyethylene piping, UNE 53.381 standard, and thermal insulation of pipes based on an elastomeric K-Flex elastomeric rubber shell.
Lighting	• A fluorescent lighting system with electronic ballasts with a power of 106,409 W.
Ventilation	• A ventilation system with time control. The indirect method is applied by setting 3312 ($l/(s \cdot m^2)$). • A flow rate of 50,909 l/s for the whole building.

B2 has a total built-up area of 9425 m^2 that is distributed as follows: (i) areas without conditioning, 2675 m^2, and (ii) areas conditioned by VRF, 6750 m^2.

Table 2 provides an overview of the main energy-consuming equipment and installations in Building B2 considered in this study. Building B2 is similar in terms of construction, use, orientation, and conditioned areas to Building B1, except for the energy generation system, which in Building B1 is low-temperature and condensation boilers, and Building B2 uses a VRF system.

Table 2. Main energy-consuming installations in B2.

Installations	Equipment Description
Heat generators	• (One unit) DAIKIN VRF Inverter with heat recovery, model REYQ32T, nominal power 90 kW in cooling and 100 kW in heating, COP/EER 4,02/3,52. • (One unit) DAIKIN VRF Inverter with heat recovery, model REYQ34T, nominal power 95.4 kW in cooling and 106.5 kW in heating, COP/EER 4.06/3.41. • (One unit) DAIKIN VRF Inverter with heat recovery, model REYQ36T, nominal power 101 kW in cooling and 113 kW in heating, COP/EER 3.87/3.22. • (Three units) DAIKIN VRF Inverter with heat recovery, model REYQ22T, nominal power 61.5 kW in cooling and 69 kW in heating, COP/EER 4.29/3.75. • (Two units) DAIKIN VRF Inverter with heat recovery, model REYQ30T, nominal power 83.9 kW in cooling and 94 kW in heating, COP/EER 4.12/3.43.
Distribution networks	• Underfloor heating made of polyethylene pipe model COBRAPEX of the TIEMME brand, on an insulating panel of expanded polystyrene with graphite with relief for pipe fixing (pitch 50 mm), complying with standard EN 13163. • Refrigerant. A three-pipe system through which the refrigerant circulates to the recovery boxes from where it is distributed to two pipes (liquid and gas) to each of the air conditioning units; it is made of copper insulated with an Armaflex-type tube. • Air ducts. A network of galvanized sheet metal ducts, insulated internally, connected to the air conditioners for the supply of ventilation to each of the classrooms and rooms treated in the building. They have been dimensioned with a maximum velocity, vertical ducts of 8 m/s, and floor ducts of 4 m/s, considering an equivalent pressure drop per meter of duct of 0.1 mm.c.w.
Heat delivery equipment	• Two-way and three-way linear discharge diffusers with built-in plenums. • Supply air swirl diffusers, as well as micro-nozzle plates. • Double deflection discharge grilles with regulation and a metal mounting frame. • Fixed louvers return grilles with filters of different dimensions. • Motorized variable flow regulation boxes for outside air supply and extraction to the different rooms. • System for VRF indoor units. • Air Handing Unit (AHU) system air brand with a rotary recuperator connected to the VRF system.
Lighting	• LED lighting system with an installed lighting power of 76,761 W.
Ventilation	• The system measures the CO_2 concentration, regulates the airflow, and estimates flow rates. • Basement floor 466 (l/s), ground floor 12,841 (l/s), 1st floor: 12,841 (l/s), 2nd floor: 6022 (l/s), 3rd floor: 3546 (l/s), and total 35,718 (l/s).

2.2. Developed Methodology

The annual SCOP for the winter period in 2022 in Building B2 $\left(SCOP_{year}^{2022}\right)$, conditioned by a VRF system is determined by the ratio of the specific energy demand for heating during each winter month of 2022 $\left(d_H^{2022}\right)$ to the specific electricity consumption of the VRF system during the same period $\left(e_{VRVE}^{2022}\right)$ (Equation (1)).

$$SCOP_{year}^{2022} = \frac{d_H^{2022}}{e_{VRVE}^{2022}} \quad (1)$$

To calculate the specific energy demand $\left(d_H^{2022}\right)$, hourly thermal loads were derived from monitored indoor and outdoor temperature data, obtained using calibrated sensors installed at key building locations, following the procedures outlined in UNE-EN 12831 [39]. This approach ensures an accurate representation of the building's actual heating demand. The total heating output of the VRF system is correlated with the building's thermal demand by employing the monitored data and the manufacturer's performance curve for the installed VRF system.

The specific electricity consumption of the VRF system $\left(e_{VRVE}^{2022}\right)$ was directly measured through dedicated energy meters installed on the VRF units, providing real-time consumption data for analysis. This measurement adheres to the test methodologies described in UNE-EN 14825 [40], ensuring compliance with standardized operational points and realistic load conditions.

The $SCOP_{year}^{2022}$ is calculated by weighting the $SCOP_{month}^{2022}$ values with the monthly heat demand for 2022 $\left(D_{H(month)}^{2022}\right)$. The $\left(SCOP_{month}^{RCZ}\right)$ and $\left(SCOP_{year}^{RCZ}\right)$ values are determined for the typical climatic year of the area, utilizing climate data from 2022, and subsequently generalized using climate data from the typical climatic year of the area. This generalization process involves calculating the Correction Factor (CF) (Equation (2)).

$$CF = \frac{308 - \left(T_s^{2022} + 273\right)}{308 - \left(T_s^{RCZ} + 273\right)} \quad (2)$$

Weather data from the Technology Research Institute in Castilla y León (ITACyL) [41] were used. This source provides hourly climate data. The period corresponding to the winter season in Segovia has been considered from December to April. Mean daily temperature and relative humidity values have been extracted, and monthly averages for temperature and relative humidity have been calculated for each month under investigation. Table 3 presents the values for the years under study.

Table 3. Average values per month and year with the annual records of the ITACyL Research Institute.

Month	2018		2022	
	T_s^{2018} (°C)	HR^{2018} (%)	T_s^{2022} (°C)	HR^{2022} (%)
January	3.4	90.2	1.6	80.9
February	2.6	84.3	4.4	78.8
March	5.9	80.9	7.3	83.6
April	10.1	77.2	8.7	76.3
May	13.1	71.2	16.1	63
June	17.6	73.6	19.9	52.4
July	20.4	57.6	24.4	40
August	21.3	51.6	23.1	43.5
September	18.7	58.9	16.3	61.1
October	11	70.4	14.8	66.5
November	7.2	85.9	11.2	87.8
December	4.1	93.2	4.4	89.2

According to Spanish legislation, it is established that for building locations at an altitude above sea level of 1000 m, the Reference Climate of the Zone (RCZ) is designated as D2 [42]. Dry temperature and relative humidity for each month, RCZ D2 data, are presented in Table 4.

To determine the renewable energy (E_{Ren}) from the VRF system in Building B2, we will consider the heating demand of the RCZ $\left(D_H^{RCZ}\right)$ and the $SCOP_{year}^{RCZ}$ calculated for Building B2, applying the expression provided in Directive (EU) 2018/2001 by the European Parliament and the Council [43] (Equation (3)).

$$E_{Ren} = D_H^{RCZ} * \left(1 - \frac{1}{SCOP_{year}^{RCZ}}\right) \quad (3)$$

Table 4. Average temperature and relative humidity of RCZ D2.

Month	Climate of the Zone (RCZ) (D2)	
	T_s^{RCZ} (°C)	H^{RCZ} (%)
January	4.8	74.7
February	6.4	65.4
March	8.2	62.4
April	10.5	59.1
May	14.4	58.9
June	18.2	50.4
July	22.1	42.5
August	21.7	43.7
September	18.7	52.1
October	13.7	63.9
November	8.1	71.1
December	5.2	74.1

3. Results and Discussion

The existence of two buildings with the same energy rating, located opposite each other and housing the same type of activity, in this case, university faculties, allows for the determination of specific heating demand and base electrical consumption. Leveraging this similarity, the SCOP, specific primary energy consumption, emissions, and energy recovery (ER) utilization of Building B2, which employs a VRF system for heating, are evaluated. The methodology applied to obtain specific base electrical and thermal consumption follows the framework outlined in Figure 3.

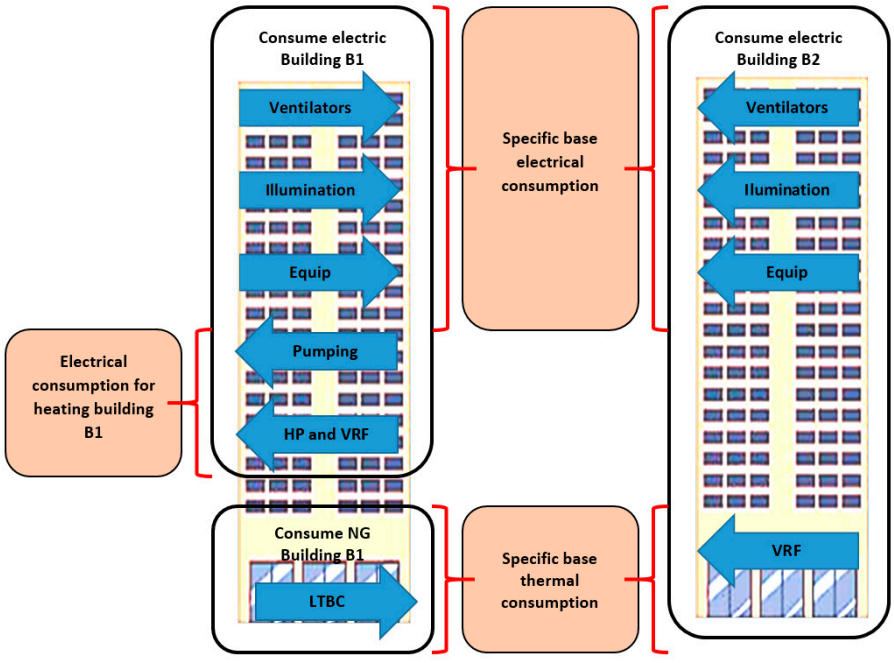

Figure 3. B1 and B2 consumption.

To conduct this study, electricity (E) and natural gas (NG) consumption data from 2018 are utilized to determine the specific base final electricity year $\left(e_{EB}^{2018}\right)$ for Building B1. Subsequently, consumption data from 2022, during which both B1 and B2 were operational, are used to determine the specific heating demand in 2022 $\left(d_H^{2022}\right)$ and specific base final electricity consumed by VRF in 2022 $\left(e_{VRVFE}^{2022}\right)$. The consumption of NG and E per month

and reference year involves the application of conversion factors between power consumption and primary energy (EP), as well as the associated CO_2 emissions from the installation. These factors are sourced from the Spanish government [44]. For conventional electricity, the primary energy-to-power consumption conversion factor is 2.403 kWh (E_p)/kWh (E_F), while the CO_2 emissions, the factor is 0.331 kg CO_2/kWh (E_F). In the case of natural gas, the conversion factor is 1.195 kWh (E_p)/kWh (E_F), with a CO_2 emissions factor of 0.252 kg CO_2/kWh (E_F).

Energy consumption (electricity and natural gas) of B1 and B2 is presented in Table 5.

Table 5. Energy consumption of Buildings B1 and B2.

Month	Electricity (B2 Building)		Natural Gas (B1 Building)	
	E_E^{2018} (kWh)	E_E^{2022} (kWh)	E_{NG}^{2018} (kWh)	E_{NG}^{2022} (kWh)
January	36,558	129,816	255,323	230,650
February	34,923	106,828	268,098	174,666
March	27,907	109,959	234,103	197,583
April	27,612	68,648	140,019	112,634
May	32,755	56,284	59,755	22,807
June	28,688	52,368	398	0
July	21,816	47,797	0	0
August	18,083	29,397	0	0
September	26,591	43,586	0	0
October	34,640	72,771	27,129	40,236
November	39,116	78,298	190,751	60,181
December	32,893	80,157	134,473	85,746
Total	372,136	862,179	1,310,049	824,086

To evaluate the electricity consumption of the campus, monitoring data were analyzed. This analysis accounts for multiple energy demands, including the electricity required for pumping thermal fluid to the air conditioning system powered by the Low-Temperature Condensing Boiler (LTCB) as well as the energy consumed by heat pumps (HPs) that condition the building's towers. Additionally, lighting-related electricity consumption is considered, noting that Building B1 is equipped with fluorescent luminaires with ballasts, which results in higher energy use compared to the LED lighting system installed in Building B2. These differences are factored into the calculations to accurately estimate and compare the base electricity consumption of both buildings. Figure 4 shows the distribution of electricity consumption for Building B1.

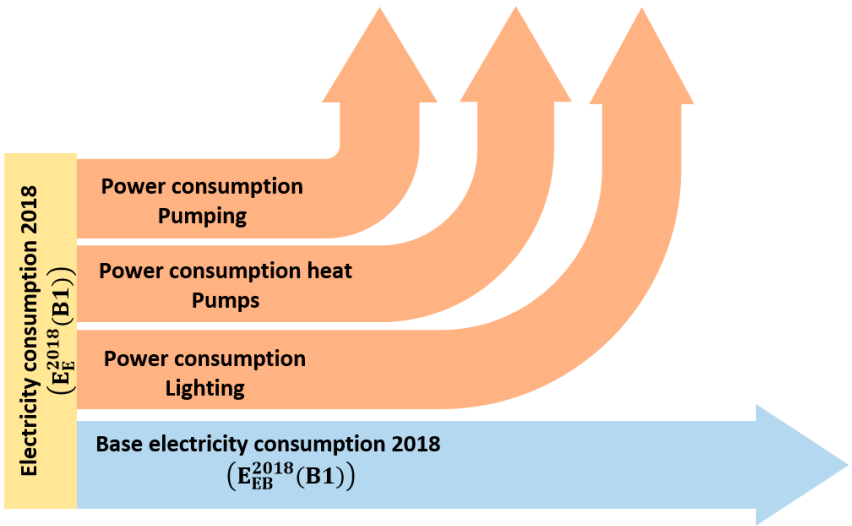

Figure 4. Distribution of B1's electricity consumption.

The excess electricity consumption due to hot water pumping from B1 $\left(E_{E-P}^{2018}\right)$ is determined based on several considerations. Firstly, the installed pumping power at the thermal plant is 4645 W, with a simultaneity factor of 0.7 [44]. Additionally, the installed pumping power for the radiant floor is 2000 W. The operation occurs during weekdays within specified periods: the winter period from 6 a.m. to 12 and 3 p.m. to 6 p.m. and the transitional period from 6 a.m. to 10 a.m. The radiant floor pumping operates 24 h a day during the winter period, while neither pumping system operates during the summer period.

The consumption for pumping is calculated on a monthly basis, considering the number of weekdays in each month and the operating hours of each pumping system. The detailed results are presented in Table 6.

Table 6. Power consumption pumping in Building B1.

Month	Working Days	Schedule	E_{E-P}^{2018} (kWh)
January	18	Winter (7 h) Radiating f. (24 h)	458
February	20	Winter (7 h) Radiating f. (24 h)	503
March	20	Winter (7 h) Radiating f. (24 h)	503
April	14	Winter (4 h) Radiating f. (24 h)	230
May	22	Summer (0 h)	-
June	21	Summer (0 h)	-
July	23	Summer (0 h)	-
August	15	Summer (0 h)	-
September	12	Summer (0 h)	-
October	22	Winter (4 h) Radiating f. (24 h)	334
November	20	Winter (7 h) Radiating f. (24 h)	503
December	12	Winter (7 h) Radiating f. (24 h)	321

The electricity consumption of the heat pumps (HP) in Building B1 $\left(E_{E-HP}^{2018}\right)$ is determined through a rigorous methodology that incorporates key factors to ensure the reliability of the estimation. First, the monthly heating energy demand per square meter for the spaces conditioned by HPs is calculated based on the natural gas consumption $\left(E_{GN}^{2018}\right)$ for the rest of the building. This approach allows for a precise correlation between energy demands in different zones of the building. Second, an efficiency factor η_{LTCB} = 0.952 is applied to account for the performance of the Low-Temperature Condensing Boiler (LTCB) system. This value reflects measured operational efficiency under real-world conditions.

Third, the heat transmission losses to the exterior, which could occur via conduction and convection, are considered negligible in this study. Specifically, we are referring to the heat transfer from the indoor (conditioned) air within the building to the outdoor environment through the building's envelope. Given that the zones heated by the heat pumps (HPs) are located within the building's interior, the losses to the exterior are minimal. This assumption is based on the fact that the building's thermal envelope provides adequate insulation, limiting the impact of external temperature fluctuations on the indoor environment. To quantify this, a reduction coefficient of 0.6 is applied, as documented in the relevant literature, which reflects the relatively low heat losses under the operational conditions of the building. This coefficient accounts for the fact that in the context of the building's design and insulation, the heat transmission to the exterior is minimal and does not significantly affect the overall energy balance [42]. These assumptions are grounded in

established thermal modeling principles and experimental validation, providing a robust basis for calculating the electricity consumption attributed to HPs in B1.

To calculate the SCOP for aerothermal energy of centralized equipment in the corresponding climatic zone, the standard UNE-EN 14285:2024 is used [40]. This involves obtaining the Power Factor (PF), which is 0.75, and CF, which is 1, for a condensation temperature of 40 °C. The SCOP results for the Mitsubishi equipment (PURY 400) are 2.820, and for the Mitsubishi equipment (PKZ-50VHAL), the result is 2.715.

The data used and the power consumption by HPs are presented in Table 7.

Table 7. Power consumption by HPs in Building B1.

Month	E_{GN}^{2018} (kWh)	d_{H}^{2018} (kWh/m^2)	D_{H-HP}^{2018} (kWh)	E_{E-HP}^{2018} (kWh)
January	255,323	43.60	32,496	11,524
February	268,098	45.78	34,122	12,100
March	234,103	39.98	29,796	10,566
April	140,019	23.91	17,821	6319
May	-	-	-	-
June	-	-	-	-
July	-	-	-	-
August	-	-	-	-
September	-	-	-	-
October	27,129	4.63	3453	1224
November	190,751	32.57	24,278	8609
December	134,473	22.96	17,115	6069

The excess consumption of the lighting system in Building B1 due to the type of luminaires is based on the following data. Firstly, Building B1 is equipped with a fluorescent lighting system with electronic ballasts, totaling 106,409 W. Secondly, Building B2 is equipped with LED lighting, with an installed lighting power of 76,761 W. A 20% overconsumption of fluorescent lights with ballasts compared to LED lights has been considered. The operating hours are determined based on the opening schedule: winter hours from 8 a.m. to 10 p.m. from Monday to Friday and summer hours from 9 a.m. to 2 p.m. Monday to Friday. A lighting switch-on simultaneity factor of 60% is applied.

Table 8 presents the annual operating hours and the excess consumption due to electronic ballasts.

Table 8. Surplus in electricity consumption in Buildings B1 and B2.

Month	Working Days	Schedule	Working Hours (h)	E_{E-L}^{2018} (kWh)
January	18	Winter (14 h)	252	3.218
February	20	Winter (14 h)	280	3.575
March	20	Winter (14 h)	280	3.575
April	14	Winter (14 h)	196	2.503
May	22	Winter (14 h)	308	3.933
June	21	Winter (14 h)	294	3.754
July	23	Summer (5 h)	115	1.468
August	15	Summer (5 h)	75	958
September	8 12	Summer (5 h) Winter (14 h)	208	2.656
October	22	Winter (14 h)	308	3.933
November	20	Winter (14 h)	280	3.575
December	12	Winter (14 h)	168	2.145

The calculated base electricity consumption is determined by subtracting the consumptions related to pumping, HP, and lighting from Building B1's electricity consumption (Table 9).

Table 9. Determination of the electricity consumption per area in Building B1.

Month	E_E^{2018} (kWh)	Extra Consumption in Building B1			E_{EB}^{2018} (kWh)	e_{EB}^{2018} (kWh/m^2)
		E_{E-P}^{2018} (kWh)	E_{E-HP}^{2018} (kWh)	E_{E-L}^{2018} (kWh)		
January	36,558	458	11,524	3218	21,358	3.10
February	34,923	503	12,100	3575	18,745	2.72
March	38,461	503	10,566	3575	23,817	3.46
April	27,612	230	6319	2503	18,560	2.69
May	-	-	-	-	-	-
June	-	-	-	-	-	-
July	-	-	-	-	-	-
August	-	-	-	-	-	-
September	-	-	-	-	-	-
October	34,640	334	1224	3933	29,149	4.23
November	39,116	503	8609	3575	26,429	3.84
December	32,893	321	6069	2145	24,358	3.54

To determine the electricity consumption of the VRF systems during the winter period in Building B2 in 2022, it is considered that the energy consumed in 2022, during which both buildings (Buildings B1 and B2) were operational, is distributed as indicated in Figure 5.

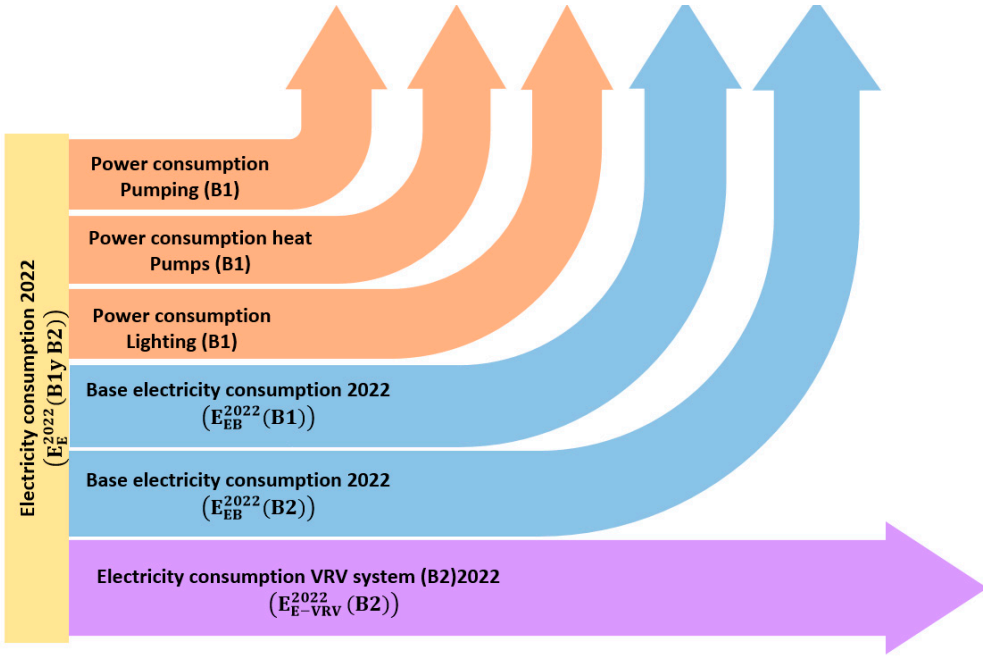

Figure 5. Electricity consumption in campus buildings (B1 and B2).

The consumptions are carried out with the same considerations as those made for determining the base consumption of B1, as described above. It is assumed that the specific base electricity consumption from 2018 will remain constant in 2022. The results of each consumption term are presented in Table 10.

Table 10. Electricity consumption in campus buildings in 2022.

Month	Consumption in B1 and B2	Consumption in B1				Consumption in B2	
	E_E^{2022} (kWh)	E_{E-P}^{2022} (kWh)	E_{E-HP}^{2022} (kWh)	E_{E-L}^{2022} (kWh)	E_{EB}^{2018} (kWh)	E_{EB}^{2018} (kWh)	E_{E-VRV}^{2022} (kWh)
January	129,816	458	11,011	3218	20,391	25,293	69,445
February	106,828	503	8339	3575	17,636	22,201	54,574
March	109,959	503	9433	3575	12,194	28,206	56,048
April	68,648	230	5377	2503	17,911	21,980	20,647
May	-	-	-	-	-	-	-
June	-	-	-	-	-	-	-
July	-	-	-	-	-	-	-
August	-	-	-	-	-	-	-
September	-	-	-	-	-	-	-
October	72,771	334	1921	3933	28,038	34,521	4024
November	78,298	503	2873	3575	25,352	31,298	14,697
December	80,157	321	4094	2145	23,698	28,842	21,057

To determine the heating demand in Building B2 for 2022 $\left(D_H^{2022}\right)$, a hybrid methodology combining monitored data and calibrated modeling was employed. The natural gas consumption for the campus in 2022 $\left(E_{NG}^{2022}\right)$, corresponding exclusively to Building B1, was used as the basis. The energy demand for heating in B1 was derived by applying the measured efficiency of the Low-Temperature Condensing Boiler (η_{LTCB}) obtained through in situ testing with a Testo brand flue gas analyzer (Model 310).

To enhance the reliability of the calculation, a calibrated energy model for Building B1 was developed and validated against the monitored gas consumption data. This model incorporates thermal properties, occupancy schedules, and local climate data to simulate building performance under the observed conditions. The specific heating demand for B1 in 2022 was then calculated based on the heated surface area and, subsequently, the same method was implemented in Building B2.

The simplified calculation process, which is presented in Figure 6, is juxtaposed with the results from the calibrated model to validate the assumptions and demonstrate the applicability of this alternative approach for similar studies. This dual-method strategy ensures that the derived heating demand values are both robust and adaptable for broader use in building energy performance analyses.

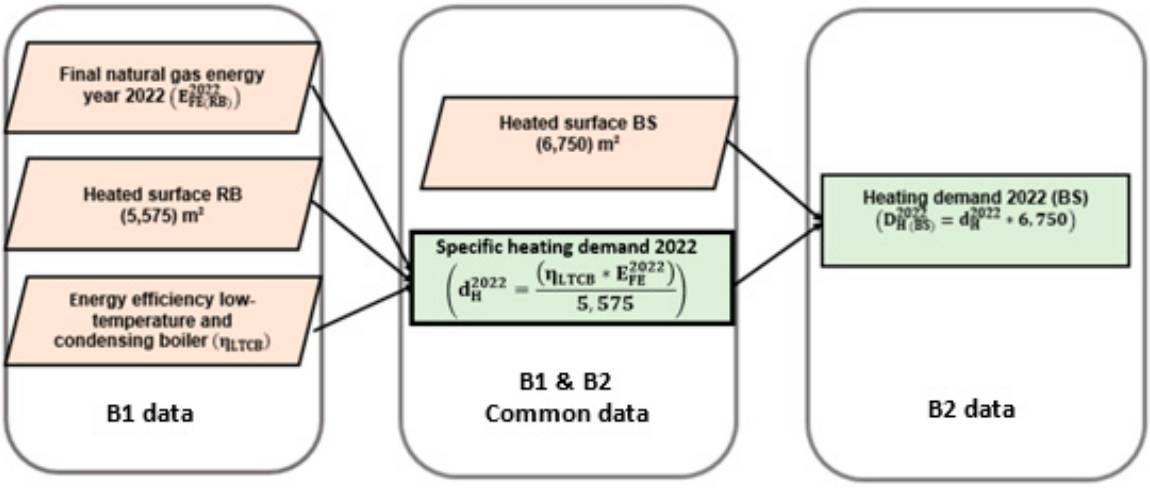

Figure 6. Building studio's heating demand calculation process.

Table 11 shows baseline data, building-specific demand, and heating demand in Building B2 in 2022.

Table 11. NG consumption, Building B1 demand, specific heating demand, and Building B2 demand.

Month	E_{NG}^{2022} (kWh)	B1 D_H^{2022} (kWh)	d_H^{2022} (kWh/m^2)	B2 D_H^{2022} (kWh)
January	230,650	219,579	39.39	321,350
February	174,666	166,282	29.83	243,350
March	197,583	188,099	33.74	275,285
April	112,634	107,228	19.23	156,930
May	-	-	-	-
June	-	-	-	-
July	-	-	-	-
August	-	-	-	-
September	-	-	-	-
October	40,236	38,305	6.87	56,060
November	60,181	57,292	10.28	83,850
December	85,746	81,630	14.64	119,464

Given the electricity consumption associated with VRF systems and the heating demand in 2022 in Building B2, the SCOP in 2022 $\left(SCOP_{month/year}^{2022}\right)$ is determined. Since the determined SCOP value corresponds to the climatic conditions of 2022, the CF for the typical climatic year in Segovia is applied and this is calculated using Equation (2).

Table 12 shows the following values for the months of the heating period: the monthly heat demand in 2022 for Building B2 $\left(D_{H\ (B2)}^{2022}\right)$, determined from the specific demand for both buildings, and electricity consumption VRF in 2022 for Building B2 $\left(E_{E\ VRV}^{2022}\right)$, which is determined by subtracting the base electricity consumption from the electricity consumption. Monthly Seasonal Coefficient of Performance (VRF) in 2022 $\left(SCOP_{month/year}^{2022}\right)$ is determined as the quotient between the heat demand and the electricity consumption in 2022. The following temperatures are recorded: Monthly Dry Temperature in 2022 $\left(T_d^{2022}\right)$ and Monthly Dry Temperature in RC $\left(T_d^{RCZ}\right)$. The SCOP is linked to the outside temperature, which allows for determining a CF coefficient, which relates SCOP to the climatic conditions, and, finally, the Monthly Seasonal Coefficient of Performance (VRF) in RCZ $\left(SCOP_{month/year}^{RCZ}\right)$ is determined.

Table 12. SCOP values of the VRF system in Building B2 in 2022 and referenced to the RCZ.

Month	$D_{H(B2)}^{2022}$ (kWh)	$\left(E_{EVRV}^{2022}\right)$ (kWh)	$SCOP_{month/year}^{2022}$ (B2 VRF)	T_d^{2022} (°C)	T_d^{RCZ} (°C)	CF	$SCOP_{month/year}^{RCZ}$ (B2 VRF)
January	321,350	69,445	4.627	1.68	4.88	0.987	4.567
February	243,350	54,574	4.459	4.44	6.41	0.992	4.423
March	275,285	56,048	4.912	7.38	8.24	0.997	4.897
April	156,930	20,647	7.601	8.75	10.55	0.993	7.547
May	-	-	-	-	-	-	-
June	-	-	-	-	---	-	-
July	-	-	-	-	--	-	-
August	-	-	-	-	-	-	-
September	-	-	-	-	-	-	-
October	56,060	4024	13.932	14.83	13.79	1.004	13.987
November	83,850	14,697	5.705	11.28	8.15	1.013	5.779
December	119,464	21,057	5.673	4.44	5.27	0.997	5.656
Year	1,256,289	240,492	5.224	7.54	8.18	1.024	5.349

VRF systems exceed the regulatory SCOP threshold of 2.5, meeting 83% of the energy demand through the use of renewable energy sources.

Building B1 is predominantly heated using a low-temperature water system with a Low-Temperature Condensing Boiler (LTCB) for climate control, which consumes NG, along with a pumping system consuming electricity. Building B2 has been equipped with a VRF system.

Considering the specific heating demand and the efficiency of the systems in Buildings B1 and B2, the specific energy consumed in each building is determined. With these values, applying the conversion factors of the Spanish Government, the specific primary energy $\left(e_P^{RCZ}\right)$ and the emissions associated $\left(gg_H^{RCZ}\right)$ with Buildings B1 and B2 are determined. In the case of Building B2, since it is a heat pump, the contribution of renewable energy $\left(e_{RE}^{RCZ}\right)$ can be determined according to Equation (3). The results are presented in Table 13.

Table 13. Summary of primary energy, emissions, and renewable energy of RE buildings.

Month	B1		B2		
	e_P^{RCZ} (kWh/m^2)	gg_H^{RCZ} (kg/m^2)	e_P^{RCZ} (kWh/m^2)	gg_H^{RCZ} (kg/m^2)	e_{RE}^{RCZ} (kWh/m^2)
January	50.56	10.65	21.11	2.91	31.33
February	45.88	9.66	19.77	2.72	28.16
March	42.75	9,00	16.63	2.29	26.96
April	29.07	6.12	7.35	1.01	20.03
May	-	-	-	-	-
June	-	-	-	-	-
July	-	-	-	-	-
August	-	-	-	-	-
September	-	-	-	-	-
October	4.37	0.91	0.58	0.08	3.13
November	38.47	8.10	12.67	1.75	25.20
December	27.06	5.70	9.11	1.26	17.66

Regarding primary energy consumption and emissions, the results obtained (Figure 7) indicate that in all cases, the primary energy consumed by the VRF system installed in Building B2 is lower than that consumed by the LTCB system installed in Building B1 throughout all heating months. Additionally, the emissions from the Building B1 system are higher than those from the Building B2 system.

By analyzing actual energy consumption, building activity, and outdoor climatic conditions during specific periods, alongside the characteristics of the facilities and their operational parameters, an assessment has been conducted regarding (i) the energy efficiency of the systems, (ii) primary energy consumption, and (iii) emissions during the heating season of a University Center situated in a warm climate zone of Europe. The key findings are summarized below. This study provides a comprehensive assessment of Variable Refrigerant Flow (VRF) systems employed in a university building during winter, presenting a critical comparison with traditional HVAC technologies, such as natural gas-fueled boiler systems. The research reveals an impressive seasonal energy efficiency value of 5.349 for the VRF system, indicating substantial energy savings and significantly reduced environmental impacts. Specifically, the findings demonstrate a 67% reduction in primary energy consumption and a 79% decrease in greenhouse gas emissions per square meter, highlighting the effectiveness of VRF systems in meeting high winter heating demands, particularly in regions with continental climates, according to Spanish Primary Energy Factors (PEFs).

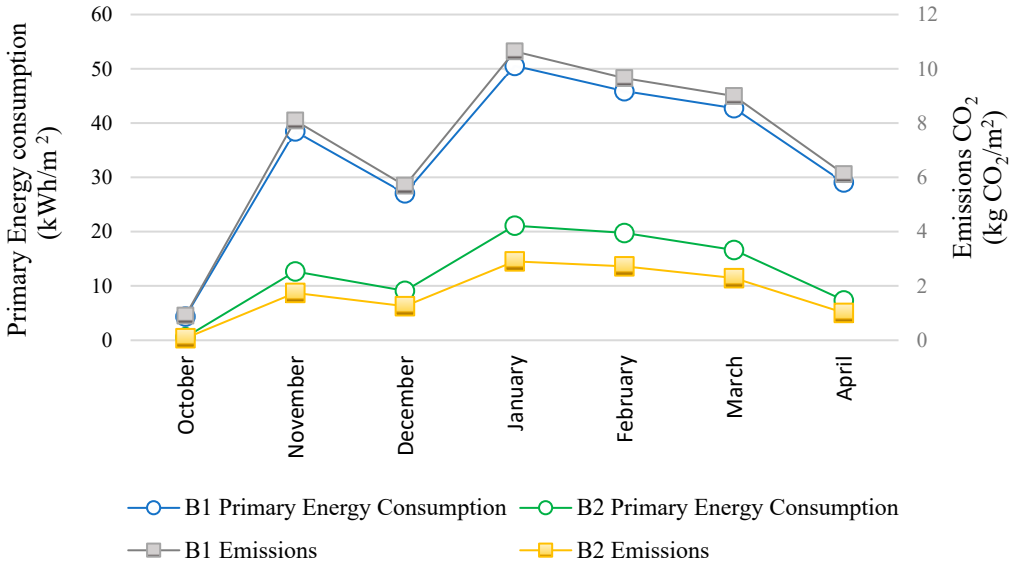

Figure 7. Primary energy consumption and emissions per area in Buildings B1 and B2.

4. Conclusions

This study provides a detailed and systematic methodology for accurately determining the real Seasonal Coefficient of Performance (SCOP) of Variable Refrigerant Flow (VRF) systems in university buildings, offering a novel approach to assess their energy efficiency and sustainability. The research focuses on a comparative analysis of two buildings with identical design parameters equipped with different HVAC systems, thereby enabling a robust evaluation of the performance of VRF systems in comparison to traditional low-temperature boiler systems, particularly in cold climates. By quantifying the real-world performance of these systems under actual operational conditions, this study offers valuable insights for building designers, facility managers, and policymakers aiming to optimize energy consumption and improve sustainability in large, energy-intensive buildings, such as universities.

The results of this study reveal a significant advantage in energy efficiency for VRF systems, with a reduction of 67% in primary energy consumption per square meter compared to conventional boiler systems. This reduction not only translates into substantial operational cost savings but also demonstrates the potential of VRF systems to optimize resource utilization, particularly in large-scale buildings with high heating demands. By leveraging advanced technologies, such as variable refrigerant flow control, VRF systems can effectively modulate energy consumption based on real-time occupancy patterns and fluctuating thermal loads, further enhancing overall system efficiency throughout the building's lifecycle. This approach enables greater flexibility and responsiveness, ensuring that energy is used only when and where it is needed, which is a crucial feature for optimizing operational costs and minimizing environmental impact.

Beyond the energy efficiency improvements, this study underscores the significant environmental benefits offered by VRF systems. The findings indicate a 79% reduction in greenhouse gas emissions (GHGs) compared to traditional boiler systems. This reduction positions VRF systems as a critical technology in the fight against climate change, aligning with global efforts to reduce the carbon footprint of the built environment. As nations and regions adopt increasingly stringent carbon reduction targets, VRF systems play a pivotal role in helping to meet these objectives. By reducing GHG emissions and contributing to national and regional climate policies, VRF systems are integral to achieving broader sustainability goals, particularly in the context of the ongoing global transition to a low-carbon economy.

In addition to energy efficiency and environmental benefits, this study highlights the capacity of VRF systems to integrate renewable energy (RE) sources into building operations. The research shows that VRF systems fulfill 83% of the building's energy demand using renewable energy, surpassing the regulatory SCOP threshold of 2.5. This accomplishment highlights the synergy between VRF systems and renewable energy sources, such as solar and geothermal energy, demonstrating that VRF systems can significantly reduce a building's reliance on non-renewable energy sources. This capability makes VRF systems an essential component of future-ready, sustainable building designs and presents a clear pathway toward achieving zero-energy buildings (ZEBs). As the global demand for sustainable building solutions grows, the integration of renewable energy with VRF technology will play a crucial role in the ongoing effort to create energy-efficient, low-carbon buildings that contribute to a sustainable future.

Furthermore, the adaptability and scalability of VRF systems offer considerable advantages in terms of system flexibility and retrofitting, particularly in existing buildings undergoing renovations or expansions. Unlike traditional HVAC systems, which often require significant overhauls or costly infrastructure changes, VRF systems can be easily integrated into buildings at various stages of their life cycle, minimizing disruption and cost. This inherent flexibility ensures that VRF systems can accommodate evolving energy demands, making them a highly attractive option for buildings that need to comply with increasingly rigorous energy efficiency standards. This feature is particularly valuable in regions characterized by harsh winters and high heating demands, such as those with continental climates and case studies where heating is a significant component of a building's total energy consumption.

This research ultimately demonstrates the strategic importance of adopting advanced HVAC technologies, such as VRF systems, as part of a comprehensive approach to addressing the challenges posed by climate change and the global need for sustainable energy solutions. The findings of this study provide compelling evidence for the adoption of VRF systems as a central technology in the transformation of the built environment toward a low-carbon, zero-energy future.

Author Contributions: Conceptualization, J.F.S.J.-A., F.J.R.-M., J.M.R.-H. and Y.A.G.; methodology, J.F.S.J.-A., F.J.R.-M., L.J.S.J.-G., A.S.-T., J.M.R.-H. and Y.A.G.; software, J.M.R.-H. and L.J.S.J.-G.; validation, J.F.S.J.-A., Y.A.G. and F.J.R.-M.; formal analysis, J.M.R.-H., J.F.S.J.-A., L.J.S.J.-G. and A.S.-T.; investigation, J.F.S.J.-A., J.M.R.-H. and A.S.-T.; resources, A.S.-T.; data curation, A.S.-T.; writing—original draft preparation, L.J.S.J.-G., J.M.R.-H. and Y.A.G.; writing—review and editing, J.F.S.J.-A., L.J.S.J.-G. and J.M.R.-H.; visualization, Y.A.G.; supervision, J.F.S.J.-A., Y.A.G. and F.J.R.-M. project administration, J.F.S.J.-A. All authors have read and agreed to the published version of the manuscript.

Funding: The financial support for this work is provided by the University of Valladolid (UVa, 18IQDF/463A303 and EUSUVA 4.0 project).

Institutional Review Board Statement: Not applicable.

Informed Consent Statement: Not applicabe.

Data Availability Statement: The original contributions presented in this study are included in the article. Further inquiries can be directed to the corresponding author.

Acknowledgments: We would like to acknowledge the University of Valladolid for providing access to the site and for facilitating this research work through the provision of equipment, space, and facilities. This paper has been made possible due to the support received by ITAP at the University of Valladolid.

Conflicts of Interest: The authors declare no conflicts of interest.

Abbreviations

AHU	Air Handing Unit
ANN	Artificial Neural Network
ARIMA	Autoregressive Integrated Moving Average
ASHP	Air Souce Heat Pump
BIM	Building Information Modeling
BREEAM	Building Research Establishment Environmental Assessment Methodology
BSA	Building Sustainability Assessment
B1	Building 1 (Reference Building)
B2	Building 2 (Building Case Study)
CF	Correction Factor
COP	Coefficient of Performance
CTE DB HE	Technical Building Code: The Basic Energy-Saving Document
D2	Name of the RCZ Under Study
d_H^{2022}	Specific Heating Demand in 2022 (kWh/m^2)
d_H^{2018}	Specific Heating Demand (B1) in 2018 (kWh/m^2)
D_H^{RCZ}	Heat Demand in RCZ (kWh)
$D_{H(month)}^{2022}$	The Monthly Heat Demand in 2022 (kWh)
$D_{H-HP(RB)}^{2018}$	The Monthly Heat Demand for the HP (B1) in 2018 (kWh)
$D_{H(month)}^{RCZ}$	The monthly Heat Demand in RCZ (kWh)
e_{EB}^{2018}	Specific Base Final Electricity in 2018 (kWh/m^2)
e_{VRV}^{2022}	Specific Base Electricity Consumption by VRF in 2022 (kWh/m^2)
e_P^{RCZ}	Specific Primary Energy Consumption for Heating in RCZ (kWh/m^2)
e_{ERH}^{RCZ}	Specifies Renewable Energy by HP in RCZ (kWh/m^2)
E_E^{2018}	Electricity Consumption in 2018 (kWh)
E_{EB}^{2018}	Base Electricity Consumption in 2018 (kWh)
E_{E-P}^{2018}	Electricity Consumption pumping in 2018 (B1) (kWh)
E_{E-HP}^{2018}	Electricity Consumption HP in 2018 (B1) (kWh)
E_{E-L}^{2018}	Electricity Consumption Lighting in 2018 (B1) (kWh)
E_E^{2022}	Electrical Energy Consumption in 2022 (kWh)
E_{EB}^{2022}	Base Electricity Consumption in 2022 (kWh)
E_{E-P}^{2022}	Electricity Consumption Pumping in 2022 (B1) (kWh)
E_{E-HP}^{2022}	Electricity Consumption HP in 2022 (B1) (kWh)
E_{E-L}^{2022}	Electricity Consumption Lighting in 2022 (B1) (kWh)
E_{E-VRV}^{2022}	Electricity Consumption VRF in 2022 (kWh)
E_{GN}^{2018}	Natural Gas Consumption in 2018 (kWh)
E_{GN}^{2022}	Natural Gas Consumption in 2022 (kWh)
E	Electricity
E_F	Final Energy (kWh)
E_P	Primary Energy (kWh)
E_{RE}	Renewable Energy (kWh)
EER	Energy Efficiency Ratio
EPCs	Energy Performance Certificates
EU	European Union
gg_H^{RCZ}	Specific Greenhouse Gas Emissions for Heating in RCZ (kg/m^2)
GHGs	Greenhouse Gases
HR^{2018}	Monthly Relative Humidity in 2018
HR^{2022}	Monthly Relative Humidity in 2022
HR^{RCZ}	Monthly Relative Humidity in RCZ

HP	Heat Pump
HULC	LIDER-CALENER Software
HVAC	Heating, Ventilation, and Air Conditioning
IEQ	Indoor Environment Quality
ITACyL	Agrarian Technological Institute of Castilla y León
MSE	Mean Squared Error
LED	Light-Emitting Diode
LEED	Leadership in Energy and Environmental Design
LTCB	Low-Temperature Condensing Boiler
MAPE	Mean Absolute Percentage Error
NG	Natural Gas
nZEB	Nearly Zero-Energy Building
PF	Power Factor
PV	Photovoltaic
RCZ	Reference Climate of the Zone
RE	Renewable Energy
RMSE	Root Mean Square Error
SCOP	Seasonal Coefficient of Performance
$SCOP_{month}^{2022}$	Monthly Seasonal Coefficient of Performance (VRF) in 2022
$SCOP_{year}^{2022}$	Annual Seasonal Coefficient of Performance (VRF) 2022
$SCOP_{month}^{RCZ}$	Monthly Seasonal Coefficient of Performance (VRF) in RCZ
$SCOP_{year}^{RCZ}$	Annual Seasonal Coefficient of Performance (VRF) In RCZ
SPF	Seasonal Performance Factor
SVM	Support Vector Machine
T_s^{2018}	Monthly Dry Temperature in 2018
T_s^{2022}	Monthly Dry Temperature in 2022
T_s^{RCZ}	Monthly Dry Temperature in RC
UBEMs	Urban Building Energy Models
US	United States
VRF	Variable Refrigerant Flow
VWV	Variable Weter Volume
η_{LTCB}	Energy Efficiency of the Low-Temperature Condensing Boiler

References

1. Directorate-General for Climate Action (European Commission). *Going Climate-Neutral by 2050—A Strategic Long-Term Vision for a Prosperous, Modern, Competitive and Climate-Neutral EU Economy*; European Commission: Brussels, Belgium, 2019; pp. 1–20.
2. European Environment Agency. *Monitoring Report on Progress Towards the 8th Environment Action Programme Objectives*; Publications Office of the European Union: Luxembourg, 2025; ISBN 9789294806154.
3. EU EPBD 2018/844/EU. Available online: https://eur-lex.europa.eu/legal-content/EN/TXT/PDF/?uri=CELEX:32018L0844&from=IT (accessed on 1 February 2024).
4. EU EPBD 2010/31/EU. Available online: https://eur-lex.europa.eu/legal-content/ES/TXT/?uri=celex:32010L0031 (accessed on 1 February 2024).
5. European Parliament. Position of the European. 2020. Available online: https://www.europarl.europa.eu/doceo/document/TA-9-2020-0010_EN.html (accessed on 1 February 2024).
6. Spain Royal Decree RD235/2013. *Boletín Oficial del Estado Spain* **2013**, *89*, 27548–27562.
7. Beltrán-Velamazán, C.; Monzón-Chavarrías, M.; López-Mesa, B. A New Approach for National-Scale Building Energy Models Based on Energy Performance Certificates in European Countries: The Case of Spain. *Heliyon* **2024**, *10*, e25473. [CrossRef] [PubMed]
8. BREEAM. Sustainable Building Certification. Available online: https://breeam.com/ (accessed on 5 March 2024).
9. LEED Certification. Available online: https://new.usgbc.org/leed (accessed on 5 March 2024).
10. Ferreira, J.; Pinheiro, M.D.; de Brito, J. Portuguese Sustainable Construction Assessment Tools Benchmarked with BREEAM and LEED: An Energy Analysis. *Energy Build.* **2014**, *69*, 451–463. [CrossRef]
11. Ferreira, A.; Pinheiro, M.D.; de Brito, J.; Mateus, R. A Critical Analysis of LEED, BREEAM and DGNB as Sustainability Assessment Methods for Retail Buildings. *J. Build. Eng.* **2023**, *66*, 105825. [CrossRef]

12. Freitas, I.A.S.; Zhang, X. Green Building Rating Systems in Swedish Market—A Comparative Analysis between LEED, BREEAM SE, GreenBuilding and Miljöbyggnad. *Energy Procedia* **2018**, *153*, 402–407. [CrossRef]
13. Gurgun, A.P.; Arditi, D. Assessment of Energy Credits in LEED-Certified Buildings Based on Certification Levels and Project Ownership. *Buildings* **2018**, *8*, 29. [CrossRef]
14. Dubljević, S.; Tepavčević, B.; Markoski, B.; Anđelković, A.S. Computational BIM Tool for Automated LEED Certification Process. *Energy Build.* **2023**, *292*, 113168. [CrossRef]
15. Alothaimeen, I.; Arditi, D.; Türkakın, O.H. Multi-Objective Optimization for LEED—New Construction Using BIM and Genetic Algorithms. *Autom. Constr.* **2023**, *149*, 104807. [CrossRef]
16. Hafez, F.S.; Sa'di, B.; Safa-Gamal, M.; Taufiq-Yap, Y.H.; Alrifaey, M.; Seyedmahmoudian, M.; Stojcevski, A.; Horan, B.; Mekhilef, S. Energy Efficiency in Sustainable Buildings: A Systematic Review with Taxonomy, Challenges, Motivations, Methodological Aspects, Recommendations, and Pathways for Future Research. *Energy Strateg. Rev.* **2023**, *45*, 101013. [CrossRef]
17. Zhao, D.; Zhong, M.; Zhang, X.; Su, X. Energy Consumption Predicting Model of VRV (Variable Refrigerant Volume) System in Office Buildings Based on Data Mining. *Energy* **2016**, *102*, 660–668. [CrossRef]
18. Pallis, P.; Braimakis, K.; Roumpedakis, T.C.; Varvagiannis, E.; Karellas, S.; Doulos, L.; Katsaros, M.; Vourliotis, P. Energy and Economic Performance Assessment of Efficiency Measures in Zero-Energy Office Buildings in Greece. *Build. Environ.* **2021**, *206*, 108378. [CrossRef]
19. Wang, R.Z.; Jin, Z.Q.; Zhai, X.Q.; Jin, C.C.; Luo, W.L.; Eikevik, T.M. Investigation of Annual Energy Performance of a VWV Air Source Heat Pump System. *Int. J. Refrig.* **2018**, *85*, 383–394. [CrossRef]
20. Gupta, G.; Mathur, S.; Mathur, J.; Nayak, B.K. Comparison of Energy-Efficiency Benchmarking Methodologies for Residential Buildings. *Energy Build.* **2023**, *285*, 112920. [CrossRef]
21. Amin, U.; Hossain, M.J.; Lu, J.; Fernandez, E. Performance Analysis of an Experimental Smart Building: Expectations and Outcomes. *Energy* **2017**, *135*, 740–753. [CrossRef]
22. Cao, L.; Li, T.; Wang, F. Heat Insulation and Thermal Insulation Method of Passive Low Energy Consumption Residential Building Exterior Envelope Structure Based on BIM. *Results Eng.* **2024**, *23*, 102734. [CrossRef]
23. Kiavarz, H.; Jadidi, M.; Rajabifard, A.; Sohn, G. An Explainable & Prescriptive Solution for Space-Based Energy Consumption Optimization Using BIM Data & Genetic Algorithm. *J. Build. Eng.* **2024**, *92*, 109763. [CrossRef]
24. Wang, D.; Pang, X.; Wang, W.; Qi, Z.; Li, J.; Luo, D. Assessment of the Potential of High-Performance Buildings to Achieve Zero Energy: A Case Study. *Appl. Sci.* **2019**, *9*, 775. [CrossRef]
25. Maboudi Reveshti, A.; Khosravirad, E.; Rouzbahani, A.K.; Fariman, S.K.; Najafi, H.; Peivandizadeh, A. Energy Consumption Prediction in an Office Building by Examining Occupancy Rates and Weather Parameters Using the Moving Average Method and Artificial Neural Network. *Heliyon* **2024**, *10*, e25307. [CrossRef]
26. Zhou, Y.; Wang, Y.; Li, C.; Ding, L.; Yang, Z. Energy-Efficiency Oriented Occupancy Space Optimization in Buildings: A Data-Driven Approach Based on Multi-Sensor Fusion Considering Behavior-Environment Integration. *Energy* **2024**, *299*, 131396. [CrossRef]
27. Mashuk, M.S.; Pinchin, J.; Siebers, P.-O.; Moore, T. Comparing Different Approaches of Agent-Based Occupancy Modelling for Predicting Realistic Electricity Consumption in Office Buildings. *J. Build. Eng.* **2024**, *84*, 108420. [CrossRef]
28. Liu, H.; Wu, Y.; Yan, D.; Hu, S.; Qian, M. Investigation of VRF System Cooling Operation and Performance in Residential Buildings Based on Large-Scale Dataset. *J. Build. Eng.* **2022**, *61*, 105219. [CrossRef]
29. Pachano, J.E.; Peppas, A.; Bandera, C.F. Seasonal Adaptation of VRF HVAC Model Calibration Process to a Mediterranean Climate. *Energy Build.* **2022**, *261*, 111941. [CrossRef]
30. Qian, M.; Yan, D.; Hong, T.; Liu, H. Operation and Performance of VRF Systems: Mining a Large-Scale Dataset. *Energy Build.* **2021**, *230*, 110519. [CrossRef]
31. Gilani, H.A.; Hoseinzadeh, S.; Karimi, H.; Karimi, A.; Hassanzadeh, A.; Garcia, D.A. Performance Analysis of Integrated Solar Heat Pump VRF System for the Low Energy Building in Mediterranean Island. *Renew. Energy* **2021**, *174*, 1006–1019. [CrossRef]
32. Zhao, D.; Zhang, X.; Zhong, M. Variable Evaporating Temperature Control Strategy for VRV System under Part Load Conditions in Cooling Mode. *Energy Build.* **2015**, *91*, 180–186. [CrossRef]
33. Liu, S.; Yu, T.; Wang, B.; Lyu, H.; Gao, R.; Shi, W. A Novel Heat Recovery VRF System: Principle and Cooling Performance Analysis. *Build. Environ.* **2024**, *266*, 112105. [CrossRef]
34. Wang, J.; Lu, X.; Adetola, V.; Louie, E. Modeling Variable Refrigerant Flow (VRF) Systems in Building Applications: A Comprehensive Review. *Energy Build.* **2024**, *311*, 114128. [CrossRef]
35. Cao, H.; Zhang, H.; Zhuang, D.; Ding, G.; Lei, J.; Huang, Z.; Li, S.; Li, J. Variable Evaporating Temperature Control Strategy for a VRF System Based on Continual Estimation of Cooling Capacity Demand of Rooms. *Energy Build.* **2024**, *305*, 113906. [CrossRef]
36. Oh, K.; Kim, E.-J. Predicting the Energy Consumption of a VRF Heat Pump Using Manufacturer Performance Data and Limited Experimentation for Dynamic Data Collection. *Energy Build.* **2024**, *303*, 113798. [CrossRef]

37. Liu, S.; Ma, G.; Lv, Y.; Xu, S. Review on Heat Pump Energy Recovery Technologies and Their Integrated Systems for Building Ventilation. *Build. Environ.* **2024**, *248*, 111067. [CrossRef]
38. Wu, Y.; Zhou, X.; Qian, M.; Jin, Y.; Sun, H.; Yan, D. Novel Approach to Typical Air-Conditioning Behavior Pattern Extraction Based on Large-Scale VRF System Online Monitoring Data. *J. Build. Eng.* **2023**, *69*, 106243. [CrossRef]
39. *UNE-EN 12381*; Energy Performance of Buildings—Method for Calculation of the Design Heat Load—Part 1: Space Heating Load, Module M3-3. Asociación Española de Normalización (AENOR): Madrid, Spain, 2019.
40. *UNE-EN 14825:2024*; Standar Air Condition, Liquid Chilling Packges and Heat Pumps, with Electrically Driven Compressors, for Space Heating and Cooling-Testing and Rating at Part Load Conditions and Calculation of Seasonal Performance. Asociación Española de Normalización (AENOR): Madrid, Spain, 2024.
41. Agricultural Technological Institute of Castilla y León (ITACyL) Agroclimatic Data. Available online: https://www.inforiego.org/opencms/opencms/info_meteo/construir/index.html (accessed on 21 February 2024).
42. CTE (Spanish Technical Building Code). Available online: http://www.codigotecnico.org (accessed on 23 September 2024).
43. Directive (EU) 2018/2001 of the European Parliament and of the Council on the Promotion of the Use of Energy from Renewable Sources. *Off. J. Eur. Union* **2018**, *2018*, 82–209.
44. Spanish Institute for Energy Saving and Diversification (IDAE). Available online: https://www.miteco.gob.es/content/dam/miteco/es/energia/files-1/Eficiencia/RITE/documentosreconocidosrite/Otros%20documentos/Factores_emision_CO2.pdf (accessed on 20 September 2024).